Homo- and Co-polymerization of Polysytrene-*block*-Poly(acrylic acid)-Coated Metal Nanoparticles

Hong Wang,[†] Xiaohui Song,[†] Cuicui Liu, Jiating He, Wen Han Chong, and Hongyu Chen*

Division of Chemistry and Biological Chemistry, Nanyang Technological University, Singapore 637371. [†]These authors contributed equally to this work.

ABSTRACT Amphiphilic block copolymers such as polystyrene-*block*-poly(acrylic acid) (PSPAA) give micelles that are known to undergo sphere-to-cylinder shape transformation. Exploiting this polymer property, core—shell nanoparticles coated in PSPAA can be "polymerized" into long chains following the chain-growth polymerization mode. This method is now extended to include a variety of different nanoparticles. A case study on the assembly process was carried out to understand the influence of the PAA block length, the surface ligand, and the size and morphology of the monomer nanoparticles. Shortening the PAA block promotes the reorganization of the amphiphilic copolymer in the micelles, which is essential for assembling large Au nanoparticles. Small Au nanoparticles can be directly "copolymerized" with empty PSPAA micelles into chains. The reaction time, acid quantity, and the [Au nanoparticles]/[PSPAA micelles] concentration ratio played important roles in controlling the sphere—cylinder—vesicle conversion of the PSPAA micelles, giving rise to different kinds of random "copolymers". With this knowledge, a general method is then developed to synthesize homo, random, and block "copolymers", where the basic units include small Au nanoparticles ($d = 16$ nm), large Au nanoparticles ($d = 32$ nm), Au nanorods, Te nanowires, and carbon nanotubes. Given the lack of means for assembling nanoparticles, advancing synthetic capabilities is of crucial importance. Our work provides convenient routes for combining nanoparticles into long-chain structures, facilitating rational design of complex nanostructures in the future.

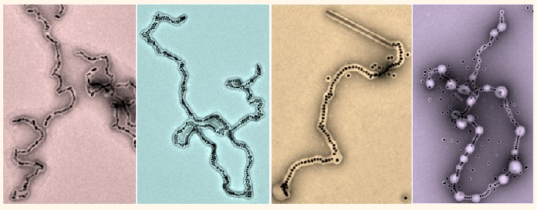

KEYWORDS: polymerization of nanoparticles · assembly · chain growth polymerization · PSPAA micelle · vesicle

Nanoparticles (NPs) are the basic building blocks in nanoscience. They can be viewed as "atoms" for constructing more complex superstructures.[1−6] While such a vision has a long history, we are far from materializing it. The field of nanoassembly is still at its infancy, where synthetic advance is the main thrust for new properties and new applications.

In assembly, the orderliness by which the components are put together is of critical importance for achieving functionality. Three-dimensional (3D) assembly can be likened to the construction of an engine from nuts and bolts, whereas 1D assembly of NPs can be compared to the polymerization of organic monomers. In terms of achieving spatial precision for building sophisticated and functional structures, the former is significantly more challenging than the latter, but even the latter has yet to be fully realized.

Given the mature field of polymer chemistry, there is great interest in following the milestones therein (synthesis of homopolymer, copolymer, dendrimer, *etc.*) for the assembly of NPs. In comparison to the 1D assembly of homologous NPs, the assembly of heterologous NPs provides a much richer structural variety, which can be explored for multifunctional and collective properties. Such heteroassembly is in a way similar to the copolymerization of organic monomers, where an enormous variety of copolymers have been synthesized for many applications. Biopolymers such as proteins and DNAs are the "crown jewels" of heteroassembly, as they are essentially precisely controlled copolymers where the structural variety leads to functional dexterity. From this perspective, new capabilities in the heteroassembly of NPs will offer novel means for exploring complex nanostructures and new properties.

In organic polymerization, the term "oligomer" typically refers to a polymer consisting of a few monomer units (<20). In this context, most of the 1D assembly of NPs in the literature is more like oligomers[7−18]

* Address correspondence to hongyuchen@ntu.edu.sg.

Received for review April 15, 2014 and accepted July 7, 2014.

Published online July 07, 2014
10.1021/nn502084a

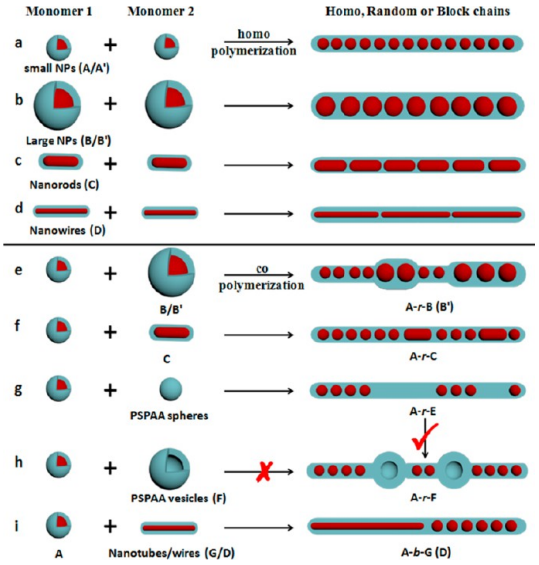

Figure 1. Schematics illustrating (a–d) the "polymerization" of core–shell NPs into "homopolymers" and (e–i) the "copolymerization" of core–shell NPs into random or block "copolymers".

than polymers.[19–21] The difficulty in obtaining long chains of NPs lies in the fact that colloidal NPs often have very similar "reactivity" (probability of successful collision) during their aggregation. As a result, their "polymerization" tends to follow the step-growth mode.[8,22] Basically, the monomers are quickly depleted, and the later stage of assembly is dominated by the collision of large clusters, which is usually difficult and nonspecific. It would be thus impractical to give orderly long chains, unless the self-assembly process is guided by a strong magnetic dipole.[23–25]

Recently, we reported an unconventional chain-growth mode in the assembly of core–shell NPs into ultralong chains.[20] The shape of polystyrene-*block*-poly(acrylic acid) (PSPAA) micelles are known to transform from sphere to cylinder upon acid treatment.[26–28] When AuNPs encapsulated in PSPAA shells (AuNP@PSPAA) were used as the monomers and subjected to acidic conditions, the PSPAA domains merged and transformed to cylindrical micelles, taking the embedded AuNPs along the way and "polymerizing" them into long chains (Figure 1). In this system, a few activated monomers were able to grow extensively into ultralong chains, whereas many monomers remained in the sample without experiencing any aggregation, indicating a chain-growth "polymerization" mode.[20,29] The presence of these monomers was essential in allowing the growth of the ultralong chains *via* sequential monomer addition.

Herein, we show that several other types of monomers can be integrated into the "polymerization" process, giving not only "homopolymers" but also random and block "copolymers" (Figure 1b–i). The viable monomers include AuNPs (d = 16 and 32 nm), Au nanorods (AuNRs), Te nanowires (TeNWs), and

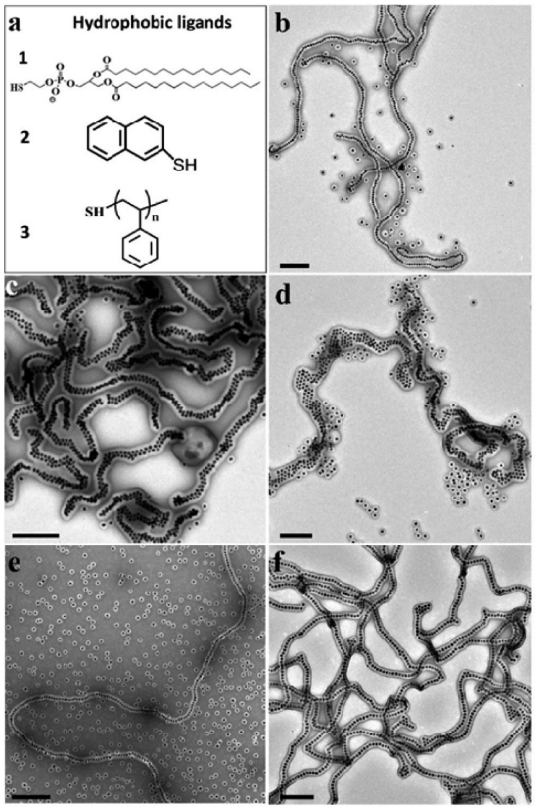

Figure 2. (a) Chemical structures of three hydrophobic ligands 1–3. (b–d) TEM images of the single-, double-, and multiple-line chains obtained in DMF/H_2O = 7:3 solution and after purification, where (b) 1-stabilized AuNPs, (c) 2-AuNPs, (d) 3-AuNPs coated in PS_{154}-*b*-PAA_{49} shells were used as the monomers. (e, f) TEM images before and after purification, when (3-AuNP)@PS_{154}-*b*-PAA_{49} were used as the monomers in DMF/H_2O = 6:1 solution. Scale bars: 200 nm.

carbon nanotubes (CNTs), all of which are encapsulated in PSPAA shells before being used in the assembly. In addition, PSPAA cylinders and vesicles can also be inserted in between the above NPs. Our new method provides a facile means to construct heteroassemblies of NPs in orderly chain configuration, where simple combination can lead to structural variety.

RESULTS AND DISCUSSION

Synthesis and Assembly. The preparation of the monomers by PSPAA encapsulation has been previously reported.[30,31] Taking the AuNP@PSPAA as an example, citrate-stabilized AuNPs were first functionalized with a layer of hydrophobic ligand (**1**, **2**, or **3**, Figure 2a), upon which the amphiphilic PSPAA self-assembled into a uniform shell. The encapsulation was carried out under high DMF content and elevated temperature, conditions which were selected to promote the mobility of the PSPAA micelles.[28,32] The hydrophobic PS blocks of the PSPAA have affinity to the hydrophobically functionalized NPs, whereas the hydrophilic PAA blocks dissolve in the solvent facing outward.[30,31] The resulting core–shell NPs were purified by centrifugation, so

that the empty PSPAA micelles (without the Au core) formed in the self-assembly can be removed.

In a typical "polymerization" process, 16 nm AuNPs encapsulated in PS_{154}-*b*-PAA_{49} shells (monomer type **A**) were used, whereby the monomers dispersed in a DMF–water mixture were treated with acid (5 mM HCl). After 2 h at 60 °C, the sample was diluted with a large amount of aq NaOH to neutralize the acid and remove DMF from the polymer shells, solidifying the polymer shells and locking the assembled chains. The final products were isolated by centrifugation and characterized by transmission electron microscopy (TEM). Typical for the chain growth "polymerization", a large number of monomers remained in the sample making it difficult to include multiple chains in each image (Figure 2e). The monomers can be readily removed in the centrifugation step, where only the ultralong chains were precipitated at a slow centrifugation speed. In the following, only the purified samples are shown in the figures.

In this system, the DMF/H_2O solvent ratio played an important role in controlling the width of the NPs chains. For example, single-line chains of AuNPs were synthesized in a DMF/H_2O = 6:1 mixture, double-line chains were obtained in DMF/H_2O = 7:3 mixture (Figure 2c), and multiple-line chains can be indirectly synthesized by treating the single-line chains in a DMF/H_2O = 3:2 mixture.[20] Here, a higher water content leads to a lesser degree of swelling in the PS domains, which in turn gives a higher PS–solvent interfacial energy[28,33] (a deswollen polymer is more dissimilar to the solvent). This leads to a larger driving force for the reduction of the surface to volume (S/V) ratio, favoring thicker chains (more longitudinal compression). In addition, swelling of the polymer domain affects the mobility of the polymer micelles, because the transformation of micelles is easier when the polymer domain is less hampered by local polymer crystallinity.[32] Typically, polymer mobility is not a limiting factor for our assembly until the water content becomes very high (e.g., DMF/H_2O = 2:3).[20]

Effects of Ligands. To optimize the conditions for "polymerizing" different types of NPs, we investigated the effects of surface ligands. In the DMF/H_2O = 7:3 mixture, the nature of ligand was found to be of importance for controlling the width of AuNP chains. Previously, double-line AuNP chains were obtained when 1,2-dipalmitoyl-*sn*-glycero-3-phosphothioethanol (a thiol-ended phospholipid, **2**, Figure 2a) was used as the ligand (Figure 2c). Under otherwise the identical conditions, when 2-naphtalenethiol (**1**) was used, single-line AuNP chains we obtained (Figure 2b); when thiol-ended polystyrene (**3**) was used, multiline AuNP chains were obtained (Figure 2d). With the same PSPAA and DMF/H_2O ratio, the polymer behavior should have been quite similar in these experiments. We speculate that the key factor is perhaps the friction among the ligand-coated AuNPs or the swelling caused by the excess ligand in the reaction mixture. More specifically, in Figure 2b, the polymer had a tendency to contract but the friction among the **1**-coated AuNPs might have prevented their reorganization. Considering the effective stacking among the rigid molecules of **1**, it is conceivable that the weaker interactions among **2** and the highly flexible PS chains in **3** might have facilitated the reorganization of the AuNPs. It is also known that homo-PS can swell the hydrophobic domain of the micelles, reducing the surface density of the PAA blocks (reducing their repulsion) and relaxing the stretching of the PS blocks in PSPAA.[31,34]

To focus on the assembly of NPs, in particular their "copolymerization", we tried to minimize the complexity of the system by avoiding the use of different surface ligands. Fortunately, stable preparative conditions can be established in the DMF/H_2O = 6:1 mixture, where single-line AuNP chains were obtained when any of the three ligands was used (Figure 2f for ligand **3**). It is likely that the higher degree of swelling by DMF leads to less polymer contraction, reducing the difference in the ligand effects. Hence, we used ligand **2** and DMF/H_2O = 6:1 mixture in most of the following experiments.

Effects of PAA Length. The above studies involved only one type of monomers, namely the 16 nm AuNPs encapsulated in PSPAA shells (monomer type **A**). If larger AuNPs (d = 32 nm) coated in PSPAA shells (type **B**) can be adapted for our assembly method, we will have two different types of monomers for their heteroassembly. However, the larger monomers were not amenable to the same assembly process, giving only short chains (Figure 3a). Most of the NPs did not participate in the aggregation, indicating a lack of progress. Prolonging the assembly time and increasing the NP concentration did not solve the problem. This is likely because that the stronger charge repulsion among the larger monomers greatly reduced the probability of effective collision. Given the same surface charge density, larger particles always have stronger charge repulsion among themselves.[10,35] While using more acid can promote the aggregation, the selectivity of 1D assembly was largely compromised, giving vesicles and irregular aggregates (similar to Figure 3c).

This problem was eventually solved by using PSPAA with shorter PAA blocks, which under similar conditions would lead to lesser surface charge density. Using 32 nm AuNPs encapsulated in PS_{144}-*b*-PAA_{22} as monomers (type **B**′), long chains of the AuNPs were obtained under the same preparative conditions (Figure 3b). Obviously, the aggregation was more extensive than that in Figure 3a. Because the NP concentration was the same, the probability of collision should be similar. Thus, the new polymer likely improved the probability of *effective* collision.

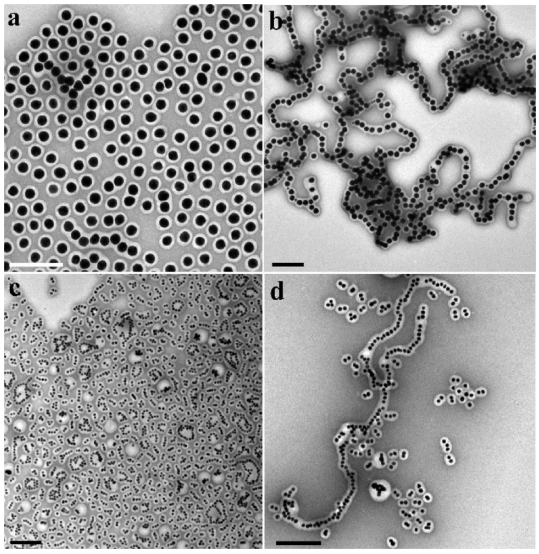

Figure 3. TEM images showing the purified products of the "homopolymerization" when (a) AuNP@PS_{154}-*b*-PAA_{49} (*d* = 32 nm, type B) and (b) AuNP@PS_{144}-*b*-PAA_{22} (*d* = 32 nm, type B′) were used as the monomers in DMF/H_2O = 6:1 solution; TEM images showing the products of the "homopolymerization" of AuNP@PS_{144}-*b*-PAA_{22} (*d* = 16 nm, type A′) in DMF/H_2O = 6:1 solution: (c) [HCl] = 5 mM, 2 h; (d) [HCl] = 0.25 mM, 25 min. Scale bars: 200 nm.

For 16 nm AuNPs in PS_{144}-*b*-PAA_{22} shells (type **A**′), the same treatment led to rapid aggregation of the monomers, giving rise to small clusters that were typical of step-growth mode (Figure 3c). As discussed above, the depletion of monomers indicates that all monomers can participate in the aggregation, as opposed to the chain-growth mode where most of them cannot. Hence, the reduction in the barrier for collision likely also reduced the selectivity of chain growth, compromising the synthetic control. Further control experiments showed that, by lowering the acid concentration and shortening the assembly time, chains of **A**′ can still be prepared (Figure 3d). The large number of dimers and trimers in this sample indicated that the aggregation was still less selective than those in Figure 2. Nevertheless, this understanding may provide a new pathway for synthesizing dimers and trimers[36] for applications in surface-enhanced Raman scattering (SERS).[37−39]

Given the faster assembly of **A**′ and **B**′ than that of **A** and **B**, the shorter PAA chains were of critical importance in promoting the effective collision, supporting our previous hypothesis in micelle aggregation.[22]

Selection of the Preparative Conditions. In summary, in this system there are quite a few controlling factors, including the solvent ratio, surface ligand, polymer chain length, acidity, temperature, and assembly time. Obviously, random search within the 6-dimension parameter space would be very difficult. Rational design is thus of crucial importance.

The solvent ratio affects the swelling of the polymer domain, whereby a higher DMF ratio leads to a higher degree of swelling and, thus, a higher mobility promoting the polymer reorganization.[32] Regarding the surface ligands, their roles are complex in affecting the interplay between the NPs and the polymer shells, as well as the interplay among the NPs in the aggregated clusters. Such a topic is of interest but beyond the scope of this work. Regarding the polymer chain length, the complex effects have been previously discussed.[40,41] In this work, only the PAA length was modulated (shortened) to facilitate NP aggregation. Regarding acidity, a higher acidity leads to a higher degree of protonation of the PAA chains, reducing charge repulsion. This affects both the kinetic barrier of aggregation (*vide supra*) and the thermodynamic end point of polymer morphology.[26,42] In this work, the same amount of acid was used to reduce the complexity of the system. Regarding to the temperature, a higher temperature leads to a higher kinetic energy, facilitating the reorganization of both the polymer chains in the micelles and the NPs in the clusters. At high temperature (>90 °C), the polymer micelles quickly evolve toward vesicles, complicating the purification of NPs. Hence, the temperature was optimized at 60 °C. Regarding to the assembly time, it affects not only the aggregation of the NPs[10] and the structural reorganization of the resulting clusters,[43,44] but also the transformation of the micelles from spheres to cylinders and then to vesicles.[45,46]

On the basis of these understandings, we optimized the conditions as follows. The solvent ratio (DMF/H_2O = 6:1) and the temperature (60 °C) were kept constant in our experiments. Ligand **2** was typically used for consistency. PS_{144}-*b*-PAA_{22} was used to promote the monomer aggregation when needed. Acidity (usually 5 mM HCl) and assembly time (typically 2 h) were used as the variables.

"Homo-Polymer" of Nanorods and Nanowires. Among the various types of nanostructures known in the literature, Au nanorods (NRs) have a unique shape that can be easily distinguished from the AuNPs. AuNRs were typically synthesized using hexadecyltrimethylammonium bromide (CTAB) as the surfactant. Being a positively charged amphiphilic molecule, it can interfere with the self-assembly of the negatively charged PSPAA. Thus, the as-synthesized AuNRs with high CTAB concentration were purified twice using centrifugation before they were used for the PSPAA encapsulation. The sample was then further purified by centrifugation to remove the empty micelles.

The resulting core−shell NPs (AuNR@PS_{154}-*b*-PAA_{49}, with ligand **2** as the surface ligand) were used as the monomer **C**. "Homo-polymerization" of **C** gave chains of AuNRs as shown in Figure 4a, where most of the AuNRs were aligned end-to-end along the longitudinal direction. Only in a few cases where the neighboring AuNRs were arranged in an end-to-side configuration. This end-to-end selectivity is likely due

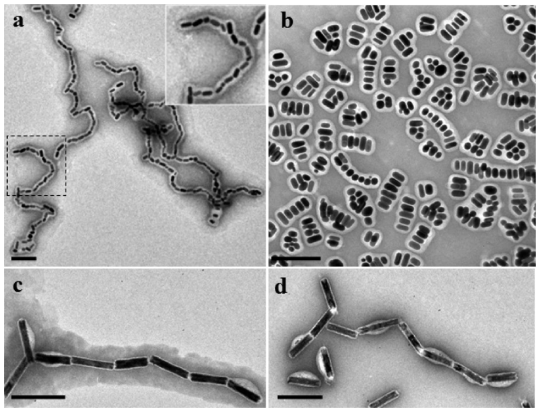

Figure 4. (a, b) TEM images showing the purified products obtained by the "homo-polymerization" of AuNR@PSPAA, where 2 (a) and 3 (b) were used as the ligands for the AuNRs. (c, d) TEM images of the purified products of the "homo-polymerization" when the TeNW@PSPAA (type D) were used as the monomers. Scale bars: 200 nm.

to (a) the higher curvature of the polymer domain at the ends, which leads to higher activity of the polymer;[33,47] and (b) the lesser charge repulsion of the end-to-end aggregation than that of end-to-side aggregation.[10] Interestingly, when ligand **3** was used for making the monomer **C**, "homo-polymerization" led to the step-growth mode, giving small clusters with mostly side-to-side configuration (Figure 4b). Compared to the results in Figure 2d, in the presence of **3**, the PSPAA micelles probably preferred a larger width, allowing the embedded AuNRs to adopt the perpendicular configuration.

We selected TeNWs as a longer alternative to the AuNRs. They were about 50 nm in diameter and 180 nm in length (Figure 4c). The as-synthesized TeNWs were purified by centrifugation to remove the surfactant sodium dodecyl sulfate (SDS) used in the synthesis.[48] They were then encapsulated in PSPAA shells by incubating them in a DMF/H_2O = 4.5:1 mixture, where PSPAA can directly self-assembly on their hydrophobic surface without any additional ligand. After purification, resulting TeNW@PS_{154}-*b*-PAA_{49} was used as the monomer **D**. Upon acid treatment, the TeNWs assembled into chains with selective end-to-end configuration (Figure 4c,d).

Random "Copolymers" of NPs. With two types of monomers **A** and **B**, we now investigate their "copolymerization". Directly mixing the monomers in the process ([**A**]:[**B**] was roughly 1:1 in the number of NPs) gave a random "copolymer" (**A**-*r*-**B**, Figure 5a). Only a few **B** NPs were incorporated in the chains (**A**:**B** = 61:1), and the remaining monomers contained mostly **B** NPs. Given the roughly equal concentration of **A** and **B**, this result further indicates that the larger **B** NPs have a lower tendency toward aggregation. After differential centrifugation to remove the monomers, the low content of **B** in the resulting "copolymer" is more evident as shown in Figure 5b.

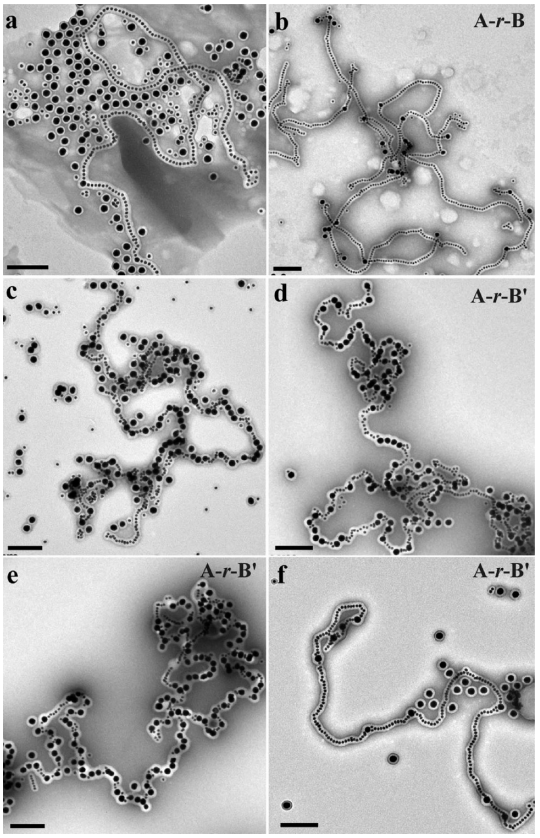

Figure 5. TEM images showing the resulting random "copolymers" synthesized from (a, b) monomer A and B ([A]/[B] = 1:1) before and after purification, respectively; (c, d) monomer A and B′ ([A]/[B′] = 1:1) before and after purification, respectively; (e) monomer A and B′, [A]/[B′] = 1:2; (f) monomer A and B′, [A]/[B′] = 2:1. Scale bars: 200 nm.

To increase the **B** content, **B**′ was used in the place of **B** for the "copolymerization". That is, **A** and **B**′ were used in a same solution, even though the monomers have different kinds of polymer shells. It was previously known that these PSPAA molecules do not readily exchange among the micelles (*i.e.*, the dissolution−remicellization process is negligible[33,49]). As shown in Figure 5c,d, when the ratio of the initial concentration was [**A**]:[**B**′] = 1:1, the "copolymerization" went well. After chain formation, a significant amount of monomers remained in the sample, indicating that the chain growth mode was still followed (Figure 5c). In contrast to Figure 5b, the higher reactivity of **B**′ led to its higher content in the resulting **A**-*r*-**B**′ chains (Figure 5d, **A**:**B**′ = 3.5:1).

The **A**/**B**′ ratio can be readily tuned by varying the concentration ratio of the monomers. As expected for a random "copolymer", when the reactivity of the monomers is kept as constant, their probability of being incorporated in the "copolymer" should be dependent on their concentration. To test this trend, the following control experiments were carried out. When the [**A**]:[**B**′] concentration ratio was decreased from 1:1 to 1:2, the resulting "copolymer" had a higher **B**′ content

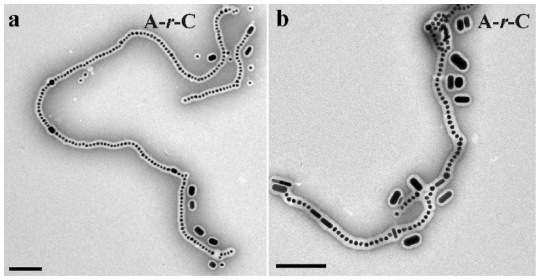

Figure 6. TEM images showing the random chains (A-*r*-C) synthesized *via* the "copolymerization" of monomer A and C: (a) ligand 2 and (b) ligand 3, respectively, were used as the surface ligands for C. Scale bars: 200 nm.

(Figure 5e, **A**:**B**′ = 1.4:1). On the other hand, when the [**A**]:[**B**′] ratio was increased to 2:1, the content of **B**′ in the "copolymer" chains was dramatically decreased (Figure 5f, **A**:**B**′ = 20:1).

Figure 6a shows the result after "co-polymerizing" **A** and **C** (random "copolymer" **A-*r*-C**, **A:C** = 42:1). Only a few AuNRs were incorporated in the resulting "copolymer", and they often align end-to-end with the neighboring AuNPs. However, our efforts to reduce the **A**:**C** ratio were not successful. While the AuNRs can be encapsulated in PS_{144}-*b*-PAA_{22} (**C**′), we were not able to use these more reactive monomers for our method.[50] Upon acid treatment, most of the monomers turned into vesicles and few participated in the "polymerization", likely due to the interference by the residue CTAB.

An initial attempt was carried out to study the self-assembly in a more complex system using different ligands. The monomers **C** were prepared using **3** as the ligand, whereas monomers **A** contained **2** as the ligand (both used PS_{154}-*b*-PAA_{49}). Mixing them in the synthesis gave long chains where most of the AuNRs adopted end-to-end configuration with the neighboring NPs (Figure 6b), although a few cases of end-to-side attachment can also be observed. Given the slow dissolution-remicellization process, there was probably negligible ligand exchange among the AuNPs and AuNRs. This result is of interest because side-to-side aggregation dominated when only monomers **C** were used for the polymerization (Figure 4b). Indeed, there were two modes even in the same sample: the AuNRs were side-to-side when aggregating with each other, but end-to-end when aggregating with the AuNPs (Figure 6b).

"Copolymers" of NPs with Cylinders/Vesicles. In comparison to the AuNPs and AuNRs, PSPAA nanostructures such as cylinders and vesicles can be more easily incorporated into the "copolymers". The simplest method is to add extra PS_{154}-*b*-PAA_{49} (2.0×10^{-6} mmol) during the "polymerization" of monomer **A**. The extra PSPAA are usually in the form of spherical micelles (Figure 7a); upon acid treatment they can aggregate and transform to cylindrical micelles,[26,28,29] which can

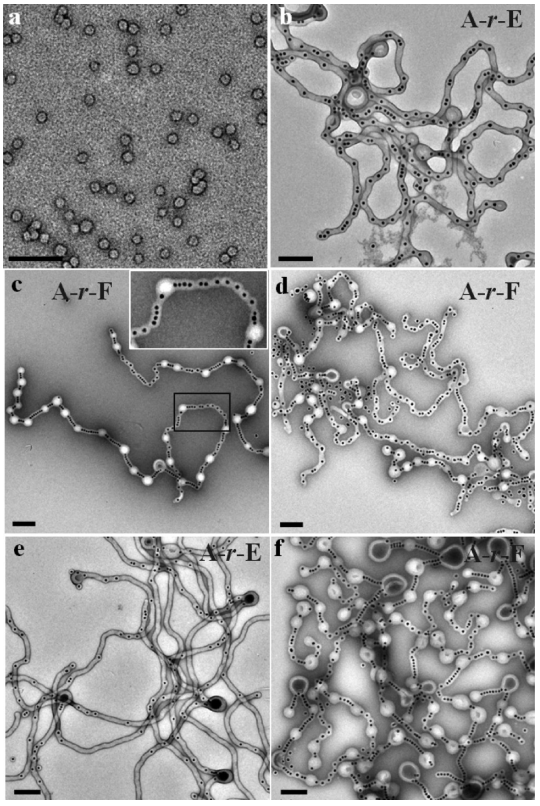

Figure 7. (a) TEM images of PSPAA spherical micelles. TEM images showing the purified random "copolymer" chains consisted of AuNP chains and PSPAA domains, which were obtained at: (b, c) 2.0×10^{-6} mmol of PSPAA, [HCl] = 5 mM, *t* = 1.5 and 6 h, respectively; (d) 2.0×10^{-6} mmol PSPAA, [HCl] = 9 mM, *t* = 1.5 h; (e, f) 4.0×10^{-6} mmol PSPAA micelles, [HCl] = 5 mM, *t* = 3 and 6 h, respectively. Scale bars: 200 nm.

be considered as another kind of monomers (type **E**). Thus, "copolymers" of AuNPs with PSPAA cylinders (**A-*r*-E**) can be obtained (5 mM HCl, 1.5 h), where both **A** and **E** are randomly incorporated in the resulting chain (Figure 7b).

For pure polymer micelles (without the embedded NPs), the assembly pathways from spherical to cylindrical micelles[28,51] have not been extensively studied. Most of the previous studies explained the phenomena from the thermodynamic perspectives that a cylinder has a lower S/V ratio (*i.e.*, lower surface energy) than the starting spheres.[46,52] Hence, the above study using AuNPs as the "markers" provides a new kinetic perspective. The spherical polymer micelles are very similar to the AuNP@PSPAA in terms of the surface PAA blocks and charge density. The side-on addition of micelles to a cylinder would obviously lead to erroneous addition of AuNPs; this mode of addition would be otherwise indistinguishable for the self-assembly of pure polymer micelles. On the basis of the similarity between the two systems, we believe that the side-on addition plays a very minor role, as compared to the end-on addition, in the growth of the pure polymer cylinders. In other words, branching is not only

thermodynamically unfavorable but also kinetically unfavorable.

It is also well-known that PSPAA cylinders can transform to vesicles where the reduction of the surface to volume ratio (S/V) of the micellar structures provides the thermodynamic driving force.[28,32] Higher temperature, longer incubation time, and more acid are known to promote the structural transformation of the micelles. Two control experiments similar to Figure 7b were carried out. In the first one, the reaction mixture was incubated for a longer period (5 mM HCl, 6 h, Figure 7c), whereas in the second experiment, more acid was added in the reaction mixture (9 mM HCl, 1.5 h, Figure 7d). In the resulting samples, most of the cylindrical PSPAA domains turned into vesicles. Only very short cylindrical sections remained (inset of Figure 7c), probably due to insufficient material to make vesicles. The vesicular moieties can be viewed as yet another type of monomer units (type **F**), making the composite chains "copolymers" of AuNPs and vesicles (**A**-*r*-**F**).

However, PSPAA vesicles cannot be directly used as the monomers for the "copolymerization" with **A**. We synthesized PSPAA vesicles of about 200 nm in diameter using a previously reported method.[28] After purification, these vesicles were mixed with **A** and they were subjected to the "copolymerization" conditions. Only "homopolymers" of **A** were obtained, and very few vesicles participated in the assembly.[50] We speculate that the vesicles are less prone to the aggregation process because they are large and thermodynamically stable.

The random copolymer of **A**-*r*-**E** can be easily tuned by varying the ratio of **A** to the extra PSPAA micelles. When the extra PSPAA amount was doubled (4.0×10^{-6} mmol), the average length of the cylindrical sections was obviously increased in the resulting chain (Figure 7e). After prolonged incubation (6 h), this sample turned into random "copolymer" **A**-*r*-**F**, where most of the cylindrical sections were converted to vesicles (Figure 7f). The resulting vesicular moieties were polydispersed in size, but they were in general larger than those in Figure 7c. The wide size distribution of the vesicles is probably a result of the wide length distribution of the cylindrical sections in the initial step. Our group previously studied the conversion of cylindrical to vesicular micelles.[32] With the inserted AuNPs serving as markers here, the selective conversion of the cylindrical sections provides additional evidence that the process proceeds without external input of materials or dramatic restructuring of the micelles. The results thus support our previously proposed kinetic pathway for the cylinder-to-vesicle transformation.

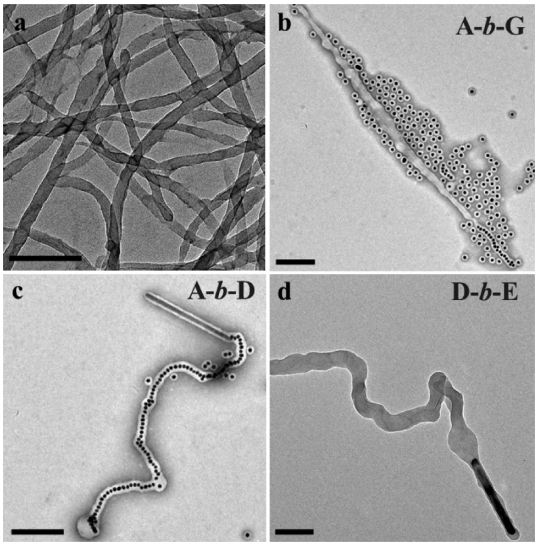

Figure 8. TEM images showing (a) CNT@PSPAA monomers (type G); (b) the block copolymer chains obtained *via* the "copolymerization" of A and G; (c, d) the block "copolymer" chains obtained *via* the "copolymerization" of (c) A with D; and (d) D with E. Scale bars: 200 nm.

"Block Copolymer" of Nanowires with NPs. To fabricate longer building blocks for the "copolymerization", we used CNTs and TeNWs with a large aspect ratio (l = 400 nm; d = 50 nm). CNT bundles of about 20 nm in width and 0.3−5 μm in length were dispersed in DMF and then encapsulated in PS_{154}-*b*-PAA_{49} shells (CNT@PSPAA, monomer **G**, Figure 8a).[53] After mixing with **A**, acid was added to induce "copolymerization". "Block copolymers" of **A**-*b*-**G** were obtained (Figure 8b), though with a low yield. Among the products, there was a significant amount of "homopolymers" of **A**. During the process, the collision between **G** and **A** is much less probable than the collision between **A** and **A**, due to the difference in their concentration. Though the tip of **G** appears to be sharp, with a much higher curvature than its side, it is not comparable to the curvature of the PSPAA shells on the small AuNPs.

Similarly, TeNW@PSPAA (monomer **D**) was also used for the "copolymerization", giving block "copolymers" **A**-*b*-**D** (Figure 8c). "Copolymerizing" **D** with extra spherical micelles (**E**) gave block "copolymers" **D**-*b*-**E** (Figure 8d).

In all these examples, the chain growth always occurred on one end of the existing block (CNT or TeNW). Typically, in the chain growth polymerization mode, most of the monomers are inactive, whereas a few are active enough to undergo extensive "polymerization" into long chains.[20] In other words, only a small percentage of the monomers were activated. Considering this low probability of activation, simultaneously activating both ends of the CNT@PSPAA or TeNW@PSPAA is highly improbable.

Thus, there is a dilemma in the synthetic design. Making the chain growth less selective (such as in Figure 3d) would lead to the step growth mode. The resulting "homopolymers" of **A** will compete with the addition of NPs to the CNT@PSPAA, limiting the length of the block "copolymers". On the other hand, making the chain growth more selective would reduce the probability of activating the ends of the CNT@PSPAA, leading to a larger percentage of unreacted CNT@PSPAA and a lower yield of the block "copolymers".

Random *versus* Block "Copolymers". Our attempts to synthesize "block copolymers" directly from the smaller monomers (AuNPs and AuNRs) were largely unsuccessful. In one of our attempts, AuNRs were first "polymerized" into chains and purified to remove most of the remaining monomers. The products were then mixed with monomers **A** to grow a second block. However, "homo-polymerization" of **A** dominated the reaction and only short blocks of **A** were found in a few cases of **A**-*b*-**C**.[50] Attempts to use the side-to-side aggregated AuNRs were also unsuccessful.

Initially, we spent great efforts optimizing the polymerization conditions, hoping to fine-tune the reactivity of the monomers *via* changes in ligand, PSPAA, or solvent conditions. However, systematic analysis of the system showed that there is no simple solution. There are major differences between the syntheses of random and block "copolymers". The former is a one-step process where the growing end remains active after each monomer addition, regardless of the type of the monomer. After reaction, the remaining monomers and short chains can be easily removed by differential centrifugation. In contrast, the synthesis of block "copolymers" requires a two-step process, where the purification after the first step is essential for removing the excess monomers. To completely exhaust the monomers in the first step reaction is not viable because the monomer concentration would be too low to complete the reaction in meaningful time frames. After the purification, however, there is a major problem in selectively activating the ends of the "polymer" for the second step growth, as discussed in the above section.

In the conventional polymerization methods, both free radicals and initiating functional groups can induce the chain growth polymerization mode. While free radicals can be used for making random copolymers, they are not the best choice for making block copolymers, which are typically synthesized by living polymerization.[54] Basically, the free radicals are not stable enough to survive the multiple steps of polymerizing the different monomers and the purification steps in between. In contrast, without chain termination, the living polymerization methods are more versatile in the synthetic design. In this sense, our method is more like free radical polymerization than living polymerization.

In comparison, an ideal method for "polymerizing" NPs has at least two requirements: (a) the end of the "polymer" chain should remain active during the "polymerization" and purification steps and (b) the monomers should not "polymerize" on their own. An alternative approach is to somehow selectively reactivate the "polymers" after purification, in order to allow the subsequent growth. These requirements are difficult to meet, because NPs typically have very similar reactivity in their aggregation. In our system, because the PSPAA shells play a critical role in controlling the NP aggregation, improving the selectivity may be still possible by designing or pretreating the PSPAA shells.

In "polymerizing" magnetic NPs, a special situation arises because the magnetic coupling is always active. One can first make magnetic chains, purify them, and then use them for growing a different kind of monomers. The main challenge here is to selectively separate the block "copolymers" from the "homopolymers". Alternatively, it is also possible to first make homopolymers of **A** and **B** separately and then couple them together into block "polymers".[55,56] Due to the difficulty in the specific **A**–**B** coupling, random coupling of the chains would give many combinations, including **AB**, **AA**, **BB**, **AAB**, **ABB**, **BAB**, **ABA**, *etc*. Also because of this problem, simply mixing monomers of **A** and **B** is not an option, as it would only give random "copolymers".

CONCLUSION

We exploited an unconventional assembly system for the "copolymerization" of nanoparticles into chain structures. The unique controls by the polymer shells and the chain growth "polymerization" mode are of critical importance for achieving the orderliness of the assembly, namely the ultralong chains with uniform width and few branches. Our understandings of the reaction parameters allowed the generic use of different nanoparticles, nanorods, and nanowires in the assembly. Further successes have been achieved in the heteroassembly of these different types of nanomaterials. Despite the orderly chain morphology, the arrangement of the nanoparticles in the chains is still far from perfect. Specifically, homo- and random-"copolymers" have been synthesized successfully, but the block-"copolymers" were only partially successful, using a single nanowire as a "block". The key problem was identified as the lack of selectivity in activating the first step "polymers" for growing the second block chains.

Nanoparticle assembly is an emerging field, where the synthetic capability is the main thrust for exploring new properties and new applications. Given the mature field of polymer chemistry and physics, borrowing

its concepts and methodology would be a convenient route for enriching the structural variety of nanoparticle assemblies, which would be essential for the future exploration.

MATERIALS AND METHODS

Materials. All chemical reagents were used without further purification. Hydrogen tetrachloroaurate(III) hydrate, 99.9% (metal basis Au 49%) was purchased from Alfa Aesar; 1,2-dipalmitoyl-*sn*-glycero-3- phosphothioethanol was purchased from Avanti Polar Lipids; amphiphilic diblock copolymer polystyrene-*block*-poly(acrylic acid) (PS_{154}-*b*-PAA_{49}, M_n = 16000 for the PS block and M_n = 3500 for the PAA block, M_w/M_n = 1.15; PS_{144}-*b*-PAA_{22}, M_n = 15000 for the PS block and M_n = 1600 for the PAA block, M_w/M_n = 1.11) were purchased from Polymer Source, Inc. Single-wall CNTs (carbonaceous purity 99%) were purchased from NanoIntegris. Hydrochloric acid was purchased from P. P. Chemicals Sdn Bhd. Deionized water (resistance > 18.2 MΩ/cm) was used in all reactions. Copper specimen grids (300 mesh) with Formvar/carbon support film were purchased from Beijing XXBR Technology Co.

The citrate-stabilized AuNPs (16, and 32 nm),[57] the CTAB-stabilized AuNRs,[58] and SDS-stabilized TeNWs[48] were prepared by following the literature produces.

Characterization. TEM images were collected on a JEM-1400 (JEOL) transmission electron microscope operated at 100–120 kV. $(NH_4)_6Mo_7O_{24}$ was used as stain (3.4 mM) in all TEM images reported in this study.

General Synthesis of NP@PSPAA Monomers. The method used here was modified from our previous report on the encapsulation of AuNPs.[30] A solution of citrate-stabilized AuNPs (d = 16 nm, 3 mL) was concentrated to ~20 μL by centrifugation at 16000*g* for 15 min. The deep red solution collected at the bottom of the eppendorf tubes was diluted with H_2O (162 μL). Then, the mixture was added to 818 μL of PSPAA solution which was prepared by mixing 738 μL DMF with PS_{154}-*b*-PAA_{49} in DMF (80 μL, 8 mg/mL).

Finally, 1,2-dipalmitoyl-*sn*-glycero-3-phosphothioethanol in EtOH (40 μL, 2 mg/mL) was added to the mixture. The final mixture has a volume of 1.04 mL with V_{DMF}/V_{H2O} = 4.5:1. It was then heated at 110 °C for 2 h and slowly cooled down until room temperature.

The same procedure was used to encapsulate AuNPs (d = 32 nm) and AuNRs with PSPAA. For the encapsulation of TeNWs, the procedure is similar to that of AuNPs, except that ligand **2** was not added.

The single-wall CNTs were dispersed into 810 μL of PSPAA solution which was prepared by mixing 730 μL DMF with PS_{154}-*b*-PAA_{49} in DMF (80 μL, 8 mg/mL) and then sonicated in an ice–water bath until to form transparent black solution. Finally, H_2O (180 μL) was added dropwise to the above solution. The final mixture has a volume of 990 μL with V_{DMF}/V_{H2O} = 4.5:1. It was then sonicated at 50 °C for 2 h and slowly cooled down until room temperature.[53]

Homoassembly of NP@PSPAA, NR@PSPAA, and NW@PSPAA into Chains. The "homo-polymerization" method used here was adapted from our previous report.[20] The purified monomers AuNP@PSPAA (d = 32 nm, type **B** and **B′**), AuNR@PSPAA (type **C**), and TeNW@PSPAA (type **D**) were dispersed into a DMF/H_2O solution (1 mL, V_{DMF}/V_{H2O} = 6:1). HCl (5 μL, 1 M) was then added into the solution, and the final concentration is $[HCl]_{final}$ = 5 mM. The mixture was incubated at 60 °C for 2 h to facilitate the shape transformation of PSPAA polymer shell.

Co-assembly of NP@PSPAA into Random Chains. The as-synthesized monomers were diluted (800 μL diluted by 11.2 mL water) and then centrifuged at 16000*g* for 30 min to remove the supernatant. The collected solution at the bottom of eppendorf tubes was diluted with NaOH (0.1 mM) and purified again. The final concentrated solution (~20 μL) contained the desired NP@PSPAA monomers free of DMF and empty PSPAA micelles. The concentrated AuNP@PSPAA (monomer **A**, d = 16 nm) and monomer **B** (AuNP@PSPAA, d = 32 nm) were dispersed into a DMF/H_2O solution (1 mL, V_{DMF}/V_{H2O} = 6:1). HCl (5 μL, 1 M) was then added into the solution, and the final concentration is $[HCl]_{final}$ = 5 mM. The mixture was incubated at 60 °C for 2 h to facilitate the shape transformation of PSPAA polymer shell. The same procedure was used when monomer **B′** and **C** were employed in the place of **B**.

The random chains consisting of monomer **A** and PSPAA vesicles were prepared using a different method. Spherical micelles of PSPAA were used. First, to PS_{154}-*b*-PAA_{49} (80 μL, 8 mg/mL) in DMF was added 738 μL DMF, and then water was added (182 μL), making a solution of V_{DMF}/V_{H2O} = 4.5:1. The polymer solution was incubated at 110 °C for 2 h and slowly cooled until room temperature. Second, the spherical PSPAA micelles (62 μL) and purified monomer **A** were simultaneously dispersed into a DMF/H_2O solution (938 μL). HCl (5 μL, 1 M) was then added into the solution, and the final concentration is $[HCl]_{final}$ = 5 mM and the final V_{DMF}/V_{H2O} = 6:1. The mixture was incubated at 60 °C for a given period of time (t = 1.5–6 h) to facilitate the shape transformation of PSPAA polymer micelles.

Co-assembly of NP@PSPAA into Block Chains. The purified CNT@PSPAA or TeNW@PSPAA was dispersed into a DMF/H_2O solution (1 mL, V_{DMF}/V_{H2O} = 6:1) containing 2 μL of HCl (1 M). The solution was heated at 60 °C for 20 min, and then the monomer **A** (AuNP@PSPAA, d = 16 nm) and HCl (1 M, 3 μL) were added. The mixture was incubated at 60 °C for 2 h to facilitate the chain growth.

Conflict of Interest: The authors declare no competing financial interest.

Acknowledgment. We thank the A*Star (SERC 112-120-2011) and MOE (RG14/13) of Singapore for financial support.

Supporting Information Available: Large-area views of TEM and support data. This material is available free of charge *via* the Internet at http://pubs.acs.org.

REFERENCES AND NOTES

1. Sau, T. K.; Murphy, C. J. Self-Assembly Patterns Formed upon Solvent Evaporation of Aqueous Cetyltrimethylammonium Bromide-Coated Gold Nanoparticles of Various Shapes. *Langmuir* **2005**, *21*, 2923–2929.
2. Lo, P. K.; Altvater, F.; Sleiman, H. F. Templated Synthesis of DNA Nanotubes with Controlled, Predetermined Lengths. *J. Am. Chem. Soc.* **2010**, *132*, 10212–10214.
3. Buck, M. R.; Schaak, R. E. Emerging Strategies for the Total Synthesis of Inorganic Nanostructures. *Angew. Chem., Int. Ed.* **2013**, *52*, 6154–6178.
4. Liu, K.; Lukach, A.; Sugikawa, K.; Chung, S.; Vickery, J.; Therien-Aubin, H.; Yang, B.; Rubinstein, M.; Kumacheva, E. Copolymerization of Metal Nanoparticles: A Route to Colloidal Plasmonic Copolymers. *Angew. Chem.* **2014**, *126*, 2686–2691.
5. Buck, M. R.; Bondi, J. F.; Schaak, R. E. A Total-Synthesis Framework for the Construction of High-Order Colloidal Hybrid Nanoparticles. *Nat. Chem.* **2012**, *4*, 37–44.
6. Sra, A. K.; Ewers, T. D.; Xu, Q.; Zandbergen, H.; Schaak, R. E. One-Pot Synthesis of bi-Disperse FePt Nanoparticles and Size-Selective Self-Assembly into AB2, AB5, and AB13 Superlattices. *Chem. Commun.* **2006**, 750–752.
7. Chen, G.; Wang, Y.; Tan, L. H.; Yang, M.; Tan, L. S.; Chen, Y.; Chen, H. High-Purity Separation of Gold Nanoparticle Dimers and Trimers. *J. Am. Chem. Soc.* **2009**, *131*, 4218–4219.
8. Wang, X. J.; Li, G. P.; Chen, T.; Yang, M. X.; Zhang, Z.; Wu, T.; Chen, H. Y. Polymer-Encapsulated Gold-Nanoparticle Dimers: Facile Preparation and Catalytical Application in Guided Growth of Dimeric ZnO-Nanowires. *Nano Lett.* **2008**, *8*, 2643–2647.

9. Xing, S.; Tan, L. H.; Yang, M.; Pan, M.; Lv, Y.; Tang, Q.; Yang, Y.; Chen, H. Highly Controlled Core/Shell Structures: Tunable Conductive Polymer Shells on Gold Nanoparticles and Nanochains. *J. Mater. Chem.* **2009**, *19*, 3286–3291.
10. Yang, M. X.; Chen, G.; Zhao, Y. F.; Silber, G.; Wang, Y.; Xing, S. X.; Han, Y.; Chen, H. Y. Mechanistic Investigation into the Spontaneous Linear Assembly of Gold Nanospheres. *Phys. Chem. Chem. Phys.* **2010**, *12*, 11850–11860.
11. DeVries, G. A.; Brunnbauer, M.; Hu, Y.; Jackson, A. M.; Long, B.; Neltner, B. T.; Uzun, O.; Wunsch, B. H.; Stellacci, F. Divalent Metal Nanoparticles. *Science* **2007**, *315*, 358–361.
12. DeVries, G. A.; Talley, F. R.; Carney, R. P.; Stellacci, F. Thermodynamic Study of the Reactivity of the Two Topological Point Defects Present in Mixed Self-Assembled Monolayers on Gold Nanoparticles. *Adv. Mater.* **2008**, *20*, 4243–4247.
13. Zhang, S. Z.; Kou, X. S.; Yang, Z.; Shi, Q. H.; Stucky, G. D.; Sun, L. D.; Wang, J. F.; Yan, C. H. Nanonecklaces Assembled from Gold Rods, Spheres, and Bipyramids. *Chem. Commun.* **2007**, 1816–1818.
14. Tang, Z. Y.; Kotov, N. A.; Giersig, M. Spontaneous Organization of Single CdTe Nanoparticles into Luminescent Nanowires. *Science* **2002**, *297*, 237–240.
15. Butter, K.; Bomans, P. H. H.; Frederik, P. M.; Vroege, G. J.; Philipse, A. P. Direct Observation of Dipolar Chains in Iron Ferrofluids by Cryogenic Electron Microscopy. *Nat. Mater.* **2003**, *2*, 88–91.
16. Xia, H.; Su, G.; Wang, D. Size-Dependent Electrostatic Chain Growth of pH-Sensitive Hairy Nanoparticles. *Angew. Chem., Int. Ed.* **2013**, *52*, 3726–3730.
17. Zhao, N.; Liu, K.; Greener, J.; Nie, Z.; Kumacheva, E. Close-Packed Superlattices of Side-by-Side Assembled Au-CdSe Nanorods. *Nano Lett.* **2009**, *9*, 3077–3081.
18. Sun, Z.; Ni, W.; Yang, Z.; Kou, X.; Li, L.; Wang, J. pH-Controlled Reversible Assembly and Disassembly of Gold Nanorods. *Small* **2008**, *4*, 1287–1292.
19. Shen, X.; Chen, L.; Li, D.; Zhu, L.; Wang, H.; Liu, C.; Wang, Y.; Xiong, Q.; Chen, H. Assembly of Colloidal Nanoparticles Directed by the Microstructures of Polycrystalline Ice. *ACS Nano* **2011**, *5*, 8426–8433.
20. Wang, H.; Chen, L. Y.; Shen, X. S.; Zhu, L. F.; He, J. T.; Chen, H. Y. Unconventional Chain-Growth Mode in the Assembly of Colloidal Gold Nanoparticles. *Angew. Chem., Int. Ed.* **2012**, *51*, 8021–8025.
21. Kim, B. Y.; Shim, I.-B.; Monti, O. L. A.; Pyun, J. Magnetic Self-Assembly of Gold Nanoparticle Chains Using Dipolar Core-Shell Colloids. *Chem. Commun.* **2011**, *47*, 890–892.
22. Liu, K.; Nie, Z. H.; Zhao, N. N.; Li, W.; Rubinstein, M.; Kumacheva, E. Step-Growth Polymerization of Inorganic Nanoparticles. *Science* **2010**, *329*, 197–200.
23. Korth, B. D.; Keng, P.; Shim, I.; Bowles, S. E.; Tang, C.; Kowalewski, T.; Nebesny, K. W.; Pyun, J. Polymer-Coated Ferromagnetic Colloids from Well-Defined Macromolecular Surfactants and Assembly into Nanoparticle Chains. *J. Am. Chem. Soc.* **2006**, *128*, 6562–6563.
24. Keng, P. Y.; Shim, I.; Korth, B. D.; Douglas, J. F.; Pyun, J. Synthesis and Self-Assembly of Polymer-Coated Ferromagnetic Nanoparticles. *ACS Nano* **2007**, *1*, 279–292.
25. Chong, W. H.; Chin, L. K.; Tan, R. L. S.; Wang, H.; Liu, A. Q.; Chen, H. Stirring in Suspension: Nanometer-Sized Magnetic Stir Bars. *Angew. Chem., Int. Ed.* **2013**, 8570–8573.
26. Zhang, L. F.; Yu, K.; Eisenberg, A. Ion-Induced Morphological Changes in "Crew-Cut" Aggregates of Amphiphilic Block Copolymers. *Science* **1996**, *272*, 1777–1779.
27. Zhang, L.; Eisenberg, A. Morphogenic Effect of Added Ions on Crew-Cut Aggregates of Polystyrene-b-poly(acrylic acid) Block Copolymers in Solutions. *Macromolecules* **1996**, *29*, 8805–8815.
28. Liu, C. C.; Chen, G.; Sun, H.; Xu, J.; Feng, Y. H.; Zhang, Z.; Wu, T.; Chen, H. Y. Toroidal Micelles of Polystyrene-block-Poly(acrylic acid). *Small* **2011**, *7*, 2721–2726.
29. Zhang, L.; Eisenberg, A. Thermodynamic *vs* Kinetic Aspects in the Formation and Morphological Transitions of Crew-Cut Aggregates Produced by Self-Assembly of Polystyrene-b-poly(acrylic acid) Block Copolymers in Dilute Solution. *Macromolecules* **1999**, *32*, 2239–2249.
30. Chen, H. Y.; Abraham, S.; Mendenhall, J.; Delamarre, S. C.; Smith, K.; Kim, I.; Batt, C. A. Encapsulation of Single Small Gold Nanoparticles by Diblock Copolymers. *ChemPhysChem* **2008**, *9*, 388–392.
31. Wang, H.; Chen, L.; Feng, Y.; Chen, H. Exploiting Core−Shell Synergy for Nanosynthesis and Mechanistic Investigation. *Acc. Chem. Res.* **2013**, *46*, 1636–1646.
32. Liu, C.; Yao, L.; Wang, H.; Phua, Z. R.; Song, X.; Chen, H. Bridging the Gap in the Micellar Transformation from Cylinders to Vesicles. *Small* **2014**, *10*, 1332–1340.
33. Chen, L.; Shen, H. W.; Eisenberg, A. Kinetics and Mechanism of the Rod-to-Wesicle Transition of Block Copolymer Aggregates in Dilute Solution. *J. Phys. Chem. B* **1999**, *103*, 9488–9497.
34. Zhang, L. F.; Eisenberg, A. Multiple Morphologies and Characteristics of "Crew-Cut" Micelle-Like Aggregates of Polystyrene-b-poly(acrylic acid) Diblock Copolymers in Aqueous Solutions. *J. Am. Chem. Soc.* **1996**, *118*, 3168–3181.
35. Wang, Y.; Chen, G.; Yang, M. X.; Silber, G.; Xing, S. X.; Tan, L. H.; Wang, F.; Feng, Y. H.; Liu, X. G.; Li, S. Z.; *et al.* A Systems Approach towards the Stoichiometry-Controlled Hetero-Assembly of Nanoparticles. *Nat. Commun.* **2010**, *1*, 87.
36. Chen, G.; Wang, Y.; Yang, M. X.; Xu, J.; Goh, S. J.; Pan, M.; Chen, H. Y. Measuring Ensemble-Averaged Surface-Enhanced Raman Scattering in the Hotspots of Colloidal Nanoparticle Dimers and Trimers. *J. Am. Chem. Soc.* **2010**, *132*, 3644–3645.
37. Yang, M. X.; Chen, T.; Lau, W. S.; Wang, Y.; Tang, Q. H.; Yang, Y. H.; Chen, H. Y. Development of Polymer-Encapsulated Metal Nanopartictes as Surface-Enhanced Raman Scattering Probes. *Small* **2009**, *5*, 198–202.
38. Chen, T.; Wang, H.; Chen, G.; Wang, Y.; Feng, Y.; Teo, W. S.; Wu, T.; Chen, H. Hotspot-Induced Transformation of Surface-Enhanced Raman Scattering Fingerprints. *ACS Nano* **2010**, *4*, 3087–3094.
39. Feng, Y. H.; Wang, Y.; Wang, H.; Chen, T.; Tay, Y. Y.; Yao, L.; Yan, Q. Y.; Li, S. Z.; Chen, H. Y. Engineering "Hot" Nanoparticles for Surface-Enhanced Raman Scattering by Embedding Reporter Molecules in Metal Layers. *Small* **2012**, *8*, 246–251.
40. Azzam, T.; Eisenberg, A. Control of Vesicular Morphologies through Hydrophobic Block Length. *Angew. Chem. In. Ed.* **2006**, *45*, 7443–7447.
41. Terreau, O.; Luo, L. B.; Eisenberg, A. Effect of Poly(acrylic acid) Block Length Distribution on Polystyrene-b-poly(acrylic acid) Aggregates in Solution. 1. Vesicles. *Langmuir* **2003**, *19*, 5601–5607.
42. Zhang, L. F.; Eisenberg, A. Morphogenic Effect of Added Ions on Crew-Cut Aggregates of Polystyrene-b-poly(acrylic acid) Block Copolymers in Solutions. *Macromolecules* **1996**, *29*, 8805–8815.
43. Urban, A. S.; Shen, X.; Wang, Y.; Large, N.; Wang, H.; Knight, M. W.; Nordlander, P.; Chen, H.; Halas, N. J. Three-Dimensional Plasmonic Nanoclusters. *Nano Lett.* **2013**, *13*, 4399–4403.
44. Wang, T.; LaMontagne, D.; Lynch, J.; Zhuang, J.; Cao, Y. C. Colloidal Superparticles from Nanoparticle Assembly. *Chem. Soc. Rev.* **2013**, *42*, 2804–2823.
45. Mai, Y. Y.; Eisenberg, A. Self-Assembly of Block Copolymers. *Chem. Soc. Rev.* **2012**, *41*, 5969–5985.
46. Discher, D. E.; Eisenberg, A. Polymer Vesicles. *Science* **2002**, *297*, 967–973.
47. Cui, H.; Chen, Z.; Wooley, K. L.; Pochan, D. J. Origins of Toroidal Micelle Formation through Charged Triblock Copolymer Self-Assembly. *Soft Matter* **2009**, *5*, 1269–1278.
48. Lin, Z. H.; Yang, Z. S.; Chang, H. T. Preparation of Fluorescent Tellurium Nanowires at Room Temperature. *Crys. Growth Des.* **2008**, *8*, 351–357.
49. Tan, L. H.; Xing, S. X.; Chen, T.; Chen, G.; Huang, X.; Zhang, H.; Chen, H. Y. Fabrication of Polymer Nanocavities with Tailored Openings. *ACS Nano* **2009**, *3*, 3469–3474.
50. See the Supporting Information for details.

51. Burke, S. E.; Eisenberg, A. Kinetics and Mechanisms of the Sphere-to-Rod and Rod-to-Sphere Transitions in the Ternary System PS310-b-PAA(52)/Dioxane/Water. *Langmuir* **2001**, *17*, 6705–6714.
52. Wang, Y.; He, J.; Liu, C.; Chong, W. H.; Chen, H. Thermodynamics *versus* Kinetics in Nanosynthesis. *Angew. Chem., Int. Ed.* **2014**, 10.1002/anie.201402986.
53. Chen, L. Y.; Wang, H.; Xu, J.; Shen, X. S.; Yao, L.; Zhu, L. F.; Zeng, Z. Y.; Zhang, H.; Chen, H. Y. Controlling Reversible Elastic Deformation of Carbon Nanotube Rings. *J. Am. Chem. Soc.* **2011**, *133*, 9654–9657.
54. Braunecker, W. A.; Matyjaszewski, K. Controlled/Living Radical Polymerization: Features, Developments, and Perspectives. *Prog. Polym. Sci.* **2007**, *32*, 93–146.
55. Hill, L. J.; Bull, M. M.; Sung, Y.; Simmonds, A. G.; Dirlam, P. T.; Richey, N. E.; DeRosa, S. E.; Shim, I.-B.; Guin, D.; Costanzo, P. J.; *et al.* Directing the Deposition of Ferromagnetic Cobalt onto Pt-Tipped CdSe@CdS Nanorods: Synthetic and Mechanistic Insights. *ACS Nano* **2012**, *6*, 8632–8645.
56. Hill, L. J.; Richey, N. E.; Sung, Y.; Dirlam, P. T.; Griebel, J. J.; Lavoie-Higgins, E.; Shim, I.-B.; Pinna, N.; Willinger, M.-G.; Vogel, W.; *et al.* Colloidal Polymers from Dipolar Assembly of Cobalt-Tipped CdSe@CdS Nanorods. *ACS Nano* **2014**, *8*, 3272–3284.
57. Frens, G. Controlled Nucleation for the Regulation of the Particle Size in Monodisperse Gold Suspensions. *Nat. Phys. Sci.* **1973**, *241*, 20–22.
58. Gole, A.; Murphy, C. J. Azide-Derivatized Gold Nanorods: Functional Materials for "Click" Chemistry. *Langmuir* **2008**, *24*, 266–272.